2013

BrachyView, A novel inbody imaging system for HDR prostate brachytherapy: Design and Monte Carlo feasibility study

M Safavi-Naeini
University of Wollongong, mitra@uow.edu.au

Z Han
University of Wollongong, zh594@uowmail.edu.au

D Cutajar
University of Wollongong, deanc@uow.edu.au

S Guatelli
University of Wollongong, susanna@uow.edu.au

M Petasecca
University of Wollongong, marcop@uow.edu.au

See next page for additional authors

BrachyView, A novel inbody imaging system for HDR prostate brachytherapy: Design and Monte Carlo feasibility study

Abstract

Purpose: High dose rate (HDR) brachytherapy is a form of radiation therapy for treating prostate cancer whereby a high activity radiation source is moved between predefined positions inside applicators inserted within the treatment volume. Accurate positioning of the source is essential in delivering the desired dose to the target area while avoiding radiation injury to the surrounding tissue. In this paper, HDR BrachyView, a novel inbody dosimetric imaging system for real time monitoring and verification of the radioactive seed position in HDR prostate brachytherapy treatment is introduced. The current prototype consists of a 15×60 mm2 silicon pixel detector with a multipinhole tungsten collimator placed 6.5 mm above the detector. Seven identical pinholes allow full imaging coverage of the entire treatment volume. The combined pinhole and pixel sensor arrangement is geometrically designed to be able to resolve the three-dimensional location of the source. The probe may be rotated to keep the whole prostate within the transverse plane. The purpose of this paper is to demonstrate the efficacy of the design through computer simulation, and to estimate the accuracy in resolving the source position (in detector plane and in 3D space) as part of the feasibility study for the BrachyView project. Methods: Monte Carlo simulations were performed using the GEANT4 radiation transport model, with a 192Ir source placed in different locations within a prostate phantom. A geometrically accurate model of the detector and collimator were constructed. Simulations were conducted with a single pinhole to evaluate the pinhole design and the signal to background ratio obtained. Second, a pair of adjacent pinholes were simulated to evaluate the error in calculated source location. Results: Simulation results show that accurate determination of the true source position is easily obtainable within the typical one second source dwell time. The maximum error in the estimated projection position was found to be 0.95 mm in the imaging (detector) plane, resulting in a maximum source positioning estimation error of 1.48 mm. Conclusions: HDR BrachyView is a feasible design for real-time source tracking in HDR prostate brachytherapy. It is capable of resolving the source position within a subsecond dwell time. In combination with anatomical information obtained from transrectal ultrasound imaging, HDR BrachyView adds a significant quality assurance capability to HDR brachytherapy treatment systems. © 2013 American Association of Physicists in Medicine.

Disciplines

Engineering | Science and Technology Studies

Authors

M Safavi-Naeini, Z Han, D Cutajar, S Guatelli, M Petasecca, M L. F Lerch, D. Franklin, J Jakubek, S Pospisil, J Bucci, M Zaider, and Anatoly B. Rosenfeld

BrachyView, A Novel In-Body Imaging System for HDR Prostate Brachytherapy: Design and Monte Carlo Feasibility Study

M. Safavi-Naeini, Z. Han, D. Cutajar, S. Guatelli, M. Petasecca, M.L.F. Lerch

Centre for Medical Radiation Physics,

University of Wollongong, Australia

D.R. Franklin

Faculty of Engineering and Information Technology,

University of Technology, Sydney, Australia

J. Jakubek and S. Pospisil

Institute of Experimental and Applied Physics (IEAP),

Czech Technical University in Prague (CTU), Czech Republic

J. Bucci

St George Hospital Cancer Care Centre, Australia

M. Zaider

Memorial Sloan Kettering Cancer Center, U.S.A

A.B. Rosenfeld[*]

Centre for Medical Radiation Physics,

University of Wollongong, Australia

(Dated: 14 May 2013)

1

Abstract

Purpose: High dose rate (HDR) brachytherapy is a form of radiation therapy for treating prostate cancer whereby a high activity radiation source is moved between predefined positions inside applicators inserted within the treatment volume. Accurate positioning of the source is essential in delivering the desired dose to the target area while avoiding radiation injury to surrounding tissue. In this paper, *HDR BrachyView*, a novel in-body dosimetric imaging system for real time monitoring and verification of the radioactive seed position in high dose rate (HDR) prostate brachytherapy treatment is introduced. The current prototype consists of a 15×60 mm^2 silicon pixel detector with a multi-pinhole tungsten collimator placed 6.5 mm above the detector. Seven identical pinholes allow full imaging coverage of the entire treatment volume. The combined pinhole and pixel sensor arrangement is geometrically designed to be able to resolve the three-dimensional location of the source. The probe may be rotated to keep the whole prostate within the transverse plane. The purpose of this paper is to demonstrate the efficacy of the design through computer simulation, and to estimate the accuracy in resolving the source position (in detector plane and in 3D space) as part of the feasibility study for the BrachyView project.

Method: Monte Carlo simulations were performed using the GEANT4 radiation transport model, with a ^{192}Ir source placed in different locations within a prostate phantom. A geometrically accurate model of the detector and collimator were constructed. Simulations were conducted with a single pinhole to evaluate the pinhole design and the signal to background ratio (SBR) obtained. Secondly, a pair of adjacent pinholes were simulated to evaluate the error in calculated source location.

Results: Simulation results show that accurate determination of the true source position is easily obtainable within the typical one second source dwell time. The maximum error in the estimated projection position was found to be 0.95 mm in the imaging (detector) plane, resulting in a maximum source positioning estimation error of 1.48 mm.

Conclusion: HDR BrachyView is a feasible design for real-time source tracking in HDR prostate brachytherapy. It is capable of resolving the source position within a sub-second dwell time. In combination with anatomical information obtained from TRUS imaging, HDR BrachyView adds a significant quality assurance capability to HDR brachytherapy treatment systems.

PACS numbers: 87.53.Jw,87.55.N-,87.55.Qr,87.56.Fc,87.57.nj,87.57.uq

I. INTRODUCTION

Prostate cancer is currently the most common malignancy amongst men in the developed world, with an age-standardised incidence rate of 155 per 100000 and a mortality rate of 23 deaths per 100000 in 2008[1]. High dose rate (HDR) Brachytherapy is an established method for treating prostate cancer whereby a high activity source of short-range radiation (such as ^{192}Ir) is remotely moved to predefined positions within applicators such as needles or catheters that have been inserted within the treatment volume. The desired dose distribution is achieved by changing source positions and adjusting the dwell time of the source in each position. Therefore, optimal dose delivery depends, amongst other things on the accuracy of catheter placement[2]. Factors resulting in dosimetric errors which potentially affect the efficacy of treatment include anatomical changes between the time of planning and surgery, human error in measuring and entering data to the afterloader system and changes in catheter location during the treatment or from fraction to fraction[2–4]. These errors may lead to post-operative complications such as incontinence and sexual dysfunction[5,6]. Therefore, using an imaging device during the procedure may assist in accurate placement of the needles for better target coverage and reduced physical injury as well as radiation injury to critical organs.

Several alternatives to TLDs for real-time quality control (QC) in HDR brachytherapy have been proposed, mostly based on real time in-vivo dosimetry in critical organs such as the urethra and rectum followed by comparison with the planned dose. Metal oxide semiconductor field effect transistor (MOSFET) detectors have been shown to be a reliable tool for real-time absolute dose measurements in HDR brachytherapy[7–9]. Qi et al. reported on the key characteristics of a recently developed MOSFET dosimetry system (MO*Skin*[10]), including the energy and angular dependence, and measured less than 5% deviation between the measured doses and the planned doses at all sampled points[8]. Systems consisting of a plastic scintillator coupled to an optical fibre placed in the urethra and rectal wall, were shown to provide an accurate dose measurement, with an angular dependence of less than 2% and a variation in depth dose readings of less than 3%[7,11–13]. Archambault et al. have presented and validated a readout system for in-vivo dosimetry based on a charge-coupled device (CCD) with multiple plastic scintillation detector (PSD) arrays that is compatible with clinical rectal balloons[14]. While these methods perform direct dose measurements, they

4

only record the dose received at a single-point, and are unable track the source position in real time. Cartwright and Suchwerska et al. have proposed a system where an array of BrachyFOD^{TM} detectors are placed within a rectal probe to measure the dose delivered during treatment[12]. The device is capable of measuring dose delivered to different parts of the rectal wall and can track the progression of the source in one dimension (parallel to the needles) with an accuracy of 2 mm; this provides limited information about the absolute position of the source within the prostate[12]. Another QC approach verifies the source position using an external imaging device[15,16]. Duan et al. have proposed a monitoring system composed of a pinhole collimator combined with a standard radiographic screen film and an x-ray fluoroscope, capable of tracking a source with a dwell time in excess of 2 seconds[15]. However, the limited dynamic range of radiographic films makes this system incapable of resolving the source location when the dwell time is within the sub second range.

HDR BrachyView is a real-time transrectal source monitoring system, which falls in the second category of aforementioned QC devices (source tracking). It tracks the source position using projections through multiple pinholes in a tungsten collimator onto a pixelated silicon detector.The device is housed within a rigid shell made of medical grade sterilisable plastic, which is inserted in the rectum and attached to the needle implant template prior to acquiring the planning CT scan. The position of the template relative to the prostate is precisely determined during the CT scan, and this will be used as the reference point for subsequent operation of the probe. This allows the HDR BrachyView assembly to be inserted into its shell to the correct depth by an electromechanical stepper unit to ensure that the entire prostate is covered by the probe's field of view during treatment. Transrectal ultrasound (TRUS) imaging may be performed through the rigid plastic shell to monitor any anatomical change in the prostate or needle positions that may require intraoperative repositioning immediately prior to treatment and between each fraction. Finally, the TRUS probe is withdrawn and the HDR BrachyView probe inserted prior to the commencement of treatment to monitor the source placement in relation to the prostate. TRUS imaging may be repeated between fractions to account for any further anatomical changes in the prostate which may occur during treatment.

This paper is divided into four sections. Design of the HDR BrachyView probe is discussed in Section II. Monte Carlo simulations to validate the proposed design are detailed in

Section III. Results based on these simulations are presented in Section IV. A thorough analysis of the simulations along with a discussion on the potential sources of error in source reconstruction is presented in Section V. An evaluation of the initial results and future development plans are discussed in Section VI.

II.   MATERIALS AND METHODS

A.   Concept of the Proposed Probe

HDR BrachyView is a transrectal probe, consisting of a multi-pinhole tungsten collimator and a 15×60 mm^2, 256×1024 pixel silicon detector designed to track and image an ^{192}Ir HDR source within a $40 \times 40 \times 40$ mm^3 volume, 5.5 mm above the probe. ^{192}Ir emits both β and γ radiation; the therapeutic action is due to the γ-rays emitted from ^{192}Ir $\rightarrow$ ^{192}Os electron-capture decay, which results in a range of γ photon energies (effective photon energy is approximately 340 keV). Multiple images of the source are projected onto the detector plane through at least two pinholes in the tungsten collimator, and the source position is determined using a simple three dimensional triangulation method that makes use of the centres of mass of the projected images as shown in Figure 1. Since these back-projected lines do not always precisely intersect, the best estimate of the source position is the point with the minimum distance to all the back-projected lines. Only a single source is utilised for HDR brachytherapy, therefore no source matching is required.

The collimator is fabricated from a cylindrical tungsten-alloy shell (95% W, 3.5% Ni and 1.5%Cu) with an outer diameter of 24 mm. Seven double-cone pinholes are uniformly distributed along the length of the shell, with a centre-to-centre spacing of 6.5 mm. Tungsten was chosen for its high mass attenuation factor, due to the high energy of the photons emitted by the ^{192}Ir HDR source. The linear attenuation coefficient (μ) is approximately 5.2$\pm$0.1 cm^{-1} for tungsten at 340 keV. Due to spatial constraints on the size of probe (the outer diameter of the probe cannot exceed 24 mm, same as the diameter of the TRUS probe) and the minification factor required to image the source within the whole field of view (FoV), the collimator shell may have a maximum thickness of 4 mm, which blocks 86.5$\pm$0.5% of incident photons. Therefore, in addition to photons travelling directly through the pinholes (*direct photons*), 13.5$\pm$0.5% of photons incident on the collimator penetrate it (*penetrated*

6
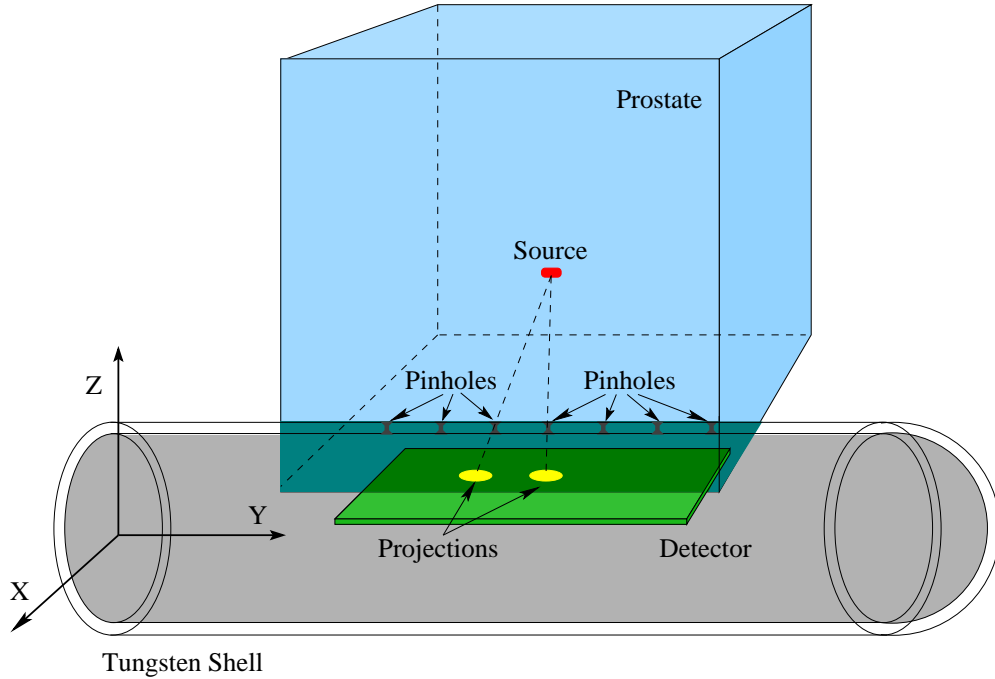
FIG. 1. Schematic diagram showing the HDR BrachyView probe relative to prostate phantom; seven equi-distant pinholes are utilised to extend the field of view to cover the whole treatment volume.

photons). This results in a background halo around the projected image, brightest directly under the source, which rapidly fades as the source moves further away.

The 256×1024 pixel detector combined with the multi-pinhole collimator extends the FoV to cover the full prostate volume in the Y-Z plane (axes shown in Figure 1). Furthermore, the probe can be rotated around its Y axis to track the source in the X-Z plane (as illustrated in Figure 1), its rotation controlled remotely and based on the expected source position and the afterloader system set up. In order to ensure that at least two projections of the source are visible from all positions within the prostate volume, seven pinholes are uniformly spaced at intervals of 6.5 mm along a straight line parallel to the Y axis of the probe. This is illustrated in Figure 2.

B. Pixelated Silicon Detector

Two main requirements determine the selection of a pixelated solid-state imaging device: high readout speed and high spatial resolution. The short source dwell time in HDR prostate

7
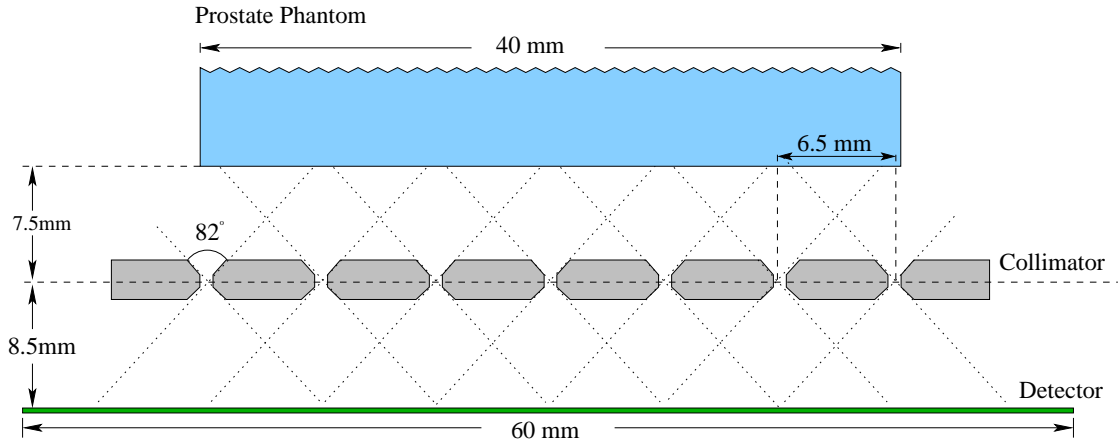
FIG. 2. Multi-pinhole collimator hole spacing.

brachytherapy requires a detector system with a sufficiently fast readout time. High detector image resolution is also critical, since as the source-to-probe distance is increased in the Z direction, its projection is "*minified*" such that the physical movement of the source is scaled to a smaller change in the position of the projection. Therefore, a high-resolution device is needed in order to achieve sufficient accuracy when the source is located near the extremities of the treatment volume.

The pixelated silicon detector *Timepix* is a newly developed variant of the well-known Medipix2 detector which satisfies these requirements[17]. Each pixel in a Timepix detector has its own preamplifier, discriminator and counter. The discriminators are used to suppress noise and select the energy range of interest. Each counter can be configured to operate in one of three modes: counting the number of detected particles, measurement of particle energy or measurement of time of interaction. Timepix is radiation-hardened and consists of 256×256 square pixels, each with an area of $55 \times 55 \ \mu m^2$. A complete imaging system can be assembled from a 4×1 array of Timepix detectors and their associated microprocessor-controlled USB readout system (Fitpix). The total sensitive detector area is $15 \times 60 \ mm^2$ (with a thickness of 500 μm). The Timepix/Fitpix system allows a frame rate rate of up to 400 images per second to be obtained with very low electronic noise[17,18].

8

(a)Cross-section of a single pinhole   (b)Pinhole dimensions
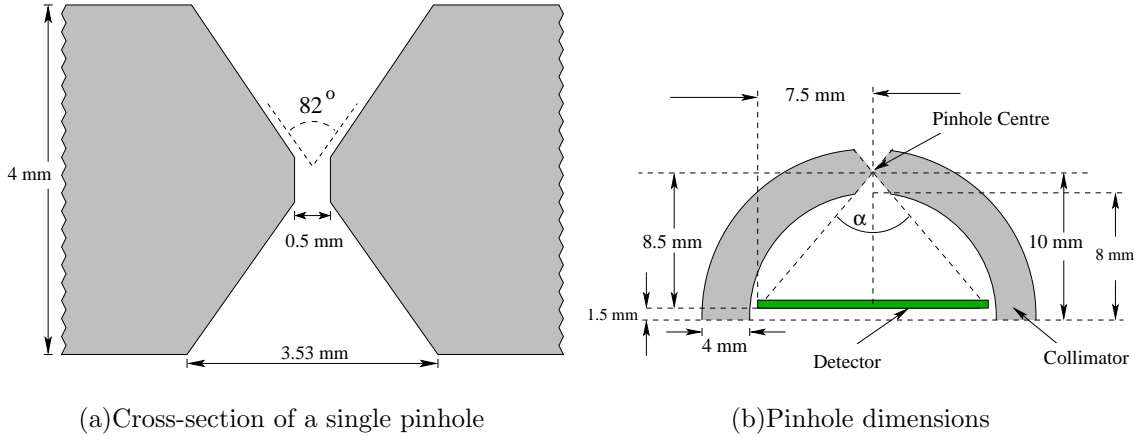
FIG. 3. Cross-section of a single pinhole. The double-cone structure was chosen to maximise the SBR over the required FoV.

C. Pinhole Geometry

The effective diameter of a pinhole in a material with a finite linear attenuation coefficient is defined as the diameter of an ideal pinhole (i.e. a pinhole cut from a material with infinite linear attenuation coefficient) which transmits the same proportion of incident photons as the given pinhole geometry fabricated from the actual collimator material[19]. The geometry chosen for the pinhole in the HDR BrachyView system is a symmetric double cone, connected by a cylindrical channel. This geometry has a smaller effective pinhole diameter compared to a single cone pinhole, which minimises photon scattering and penetration close to the aperture[19,20]. This results in a higher ratio of direct to penetrated photons (henceforth referred to as *signal to background ratio* or SBR) compared with a single-cone pinhole structure, leading to a superior system spatial resolution[21].

To maximise the field of view, the detector should be placed as close as practically possible to the pinhole collimator. However, this proximity is limited by the physical dimensions of the detector (a width of 15 mm and thickness of 0.5 mm) and the inner dimensions of the probe cavity. The detector can be placed no more than 1.5 mm above the centre of the probe cavity, the outer diameter of the probe cannot exceed 24 mm (same as the outer diameter of the TRUS probe it is replacing) and the collimator thickness is 4 mm; this results in an opening angle for the cones (α) of 82° (as illustrated in Figure 3(a)). A cylindrical channel with a diameter of 0.50 mm and length of 0.57 mm is added to simplify manufacturing of the collimator structure.
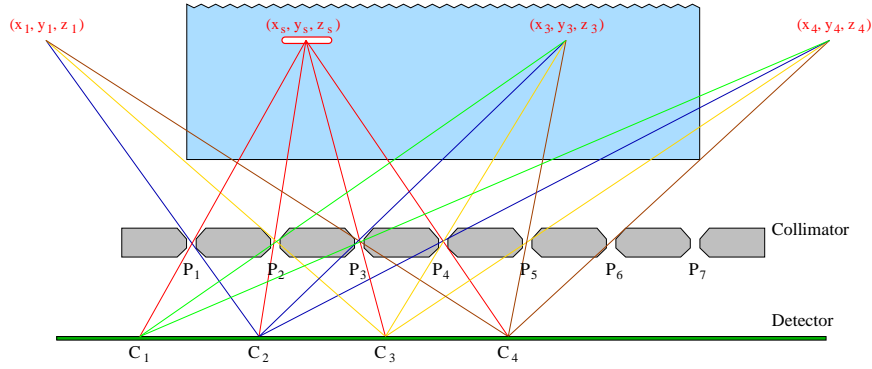
FIG. 4. Example source location with four projections visible, illustrating the ambiguity of the estimated source location; the ambiguity is resolved by considering the relative brightness of the projections.

D. Projected Image Analysis

Accurately resolving the three dimensional source location depends on the ability to distinguish between the projected image and the background contribution made by the penetrated photons. A significant fraction of the high energy photons emitted by the ^{192}Ir source with peak energies at 295.6 keV and 308.4 keV, extending up to 884.5 keV, penetrate the body of the collimator, resulting in significant count rates being registered by pixels directly below the source. This results in a reduced contrast between the projection image and the background, especially when the source approaches the edge of a pinhole's FoV - leading to a small error in the location of the centre of mass of the resulting projection. A median filter is used to reduce the speckle noise in the image. Pixels with a count rate below a certain threshold are filtered out (a threshold value of 80% was chosen to analyse projection images presented in this paper) prior to calculating the location of the centres of mass.

The projections will be approximately collinear and lie on a line which is parallel to the row of pinholes. Ideally, there will be one projection for each of the N_p pinholes, where N_p is the total number of pinholes (i.e. 7 in this instance); however when the source is very close to the collimator, this will not be the case. If the N_p projections are visible, there is no ambiguity in the three-dimensional position of the source, and its position will be the intersection of the lines drawn from the centres of mass of the seven projections through the seven pinholes, in corresponding order. However, if the source is closer to the collimator

10

and/or near the end of the detector array, it is possible that fewer than seven projections will be observed, due to the limited angle of acceptance of the pinholes and the fact that some projections will not be on the detector. The collimator placement is such that all potential source locations within the field of view will result in at least two projections of the source on the detector; that is $2 \leq N_c \leq N_p$, where N_c is the number of visible projections). Therefore, there will be $N_p - N_c + 1$ possible sets of consecutive pinholes through which the source may have been projected onto the visible spots on the detector. Each of these sets results in a different potential source position. An example where $N_c = 4$ is illustrated in Figure 4.

This ambiguity can be resolved since the intensity of the projected images will not be the same; due to the inverse square law, the brightest projections will be those at the minimum distance from the source. Therefore, either the brightest projection may be associated with its nearest pinhole, or the centre of mass of the overall image field can be used to determine which of the $N_p - N_c + 1$ possible sets of consecutive pinholes the projections have passed through. This will uniquely identify the location of the source.

III.   MONTE-CARLO SIMULATIONS

Models of a single pinhole and double pinhole tungsten collimator and HDR ^{192}Ir source were developed in a dedicated GEANT4 simulation application. A micro-Selectron HDR ^{192}Ir source (shown in Figure 5(a)) was modelled in the simulation[22]. The core consists of a pure Iridium metal cylinder with ^{192}Ir uniformly distributed along its length with a surrounding steel shell which is connected to a 2 mm long steel cable. The collimator was modelled as a cylindrical tungsten tube with a wall thickness of 4 mm and is shown in Figure 5(b). In practice, only the top half of the tube needs to be fabricated from tungsten, which also allows the lower cones to be more easily machined. The pixellated silicon detector is placed 1.5 mm above the centre of the tungsten collimator. To simplify the geometric description of the pinhole in GEANT4, the area immediately surrounding the pinhole was approximated as a trapezoidal prism (Figure5(b)).

Ten billion photon events were generated for each simulation (an added 10 billion photon events had to be generated for the source placed at maximum distance from the collimator). The photon energy distribution was generated according to the spectrum of ^{192}Ir[22]. It is assumed that all beta radiation is absorbed by the steel shell and the surrounding phan-

(a)Simulated ^{192}Ir source   (b)Simulated pinhole/collimator
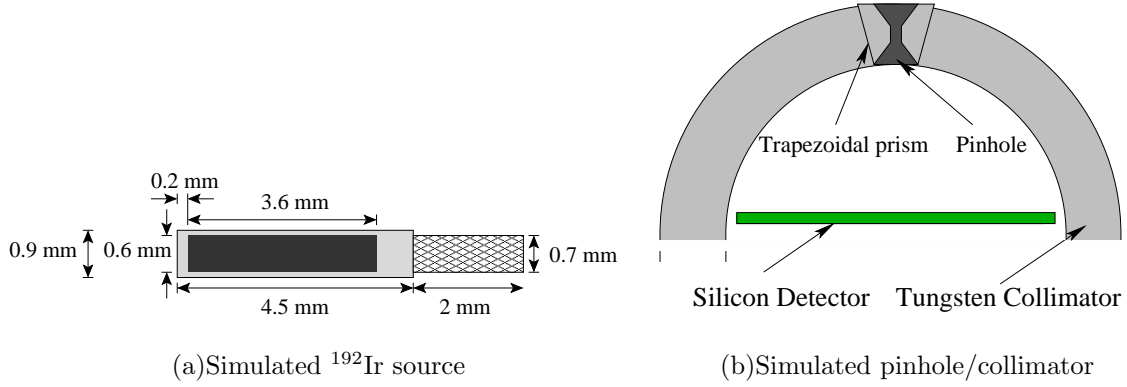
FIG. 5.   The simulated ^{192}Ir source.   The core consists of pure Iridium containing a uniform distribution of ^{192}Ir radioisotope with a surrounding steel shell;The cross section of the tungsten collimator and a single pinhole, simulated in GEANT4.

tom. The region of production of secondary particles was set from 4 mm outside the probe (tungsten tube) to 1 μm inside the probe. GEANT4 Low Energy package (G4LowEnergy package), using the Livermore Evaluated Data Libraries was employed to model the physics interactions.   The output file consists of the index of pixels and recorded counts in each pixel, where if the deposited energy in each pixel for every event exceeds 16 keV, the count is incremented by one.

Two Monte Carlo studies are detailed in the following sections. Section III A examines the effect of source position on the projected image and evaluates the minimum count rates registered by the pixellated silicon detector. In Section III B, a dual-pinhole configuration is simulated and is used to evaluate the proposed geometry of the multi-pinhole collimator and the resulting projection images. A second two pinhole simulation was conducted to estimate the error in the calculated source position within the prostate volume as a function of source position in simulated a phantom.

A.   Single-Hole Collimator, Multiple Source Positions

The effect of source position on projection image contrast and count rate was studied by simulating a single pinhole collimator and a 15×15 mm^2 pixellated detector (equivalent to a single Timepix device) with the source positioned in different locations. The simulation configuration is illustrated in Figure 6, where the source is placed above the collimator; h is the distance between the source and the pinhole centre and θ is the incidence angle measured

12

TABLE I. Primary ^{192}Ir photon energies and their respective emission probabilities per decay used in GEANT4 simulations.

Primary Energy	Emission Probability(%)
10.5 keV	2.46
64 keV	4.54
75 keV	1.22
136.5 keV	0.08
201.5 keV	0.20
205.5 keV	1.41
283.5 keV	0.11
295.5 keV	12.21
308.5 keV	12.7
316.5 keV	35.04
374.5 keV	0.30
416.5 keV	0.28
468.5 keV	20.23
484.5 keV	1.34
489.5 keV	0.18
588.5 keV	1.90
604.5 keV	3.45
612.5 keV	2.23
884.5 keV	0.12

from the pinhole plane ($\theta = 90$ is normal incidence). Eight simulations were conducted with three values of h (5 mm, 21 mm and 45 mm) and three values of θ (90°, 72°, 57°).

B. Double Pinholes

A series of simulations were performed to evaluate the ability of the proposed collimator geometry to resolve the source position at its minimum distance from the face of the probe, where the ratio of *penetrated* to *direct* photons is at its maximum. A collimator with two
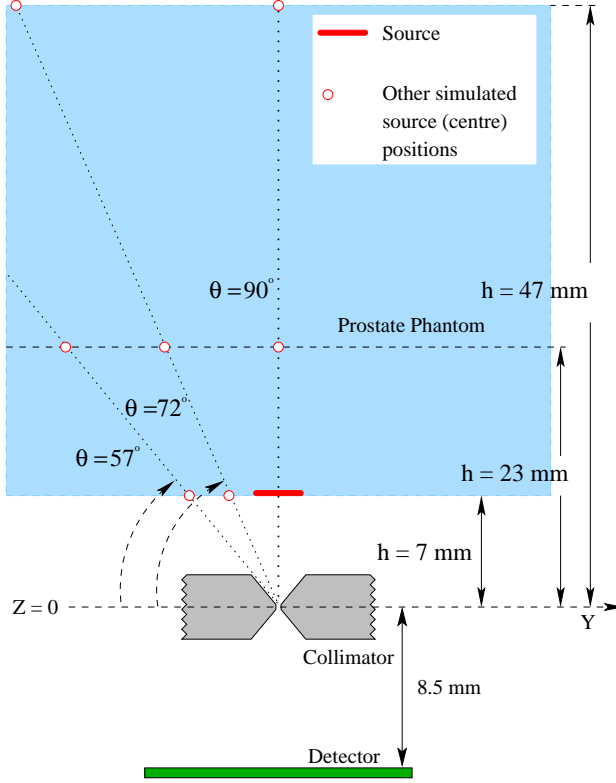
FIG. 6. Source positions for the first group of simulations. Only one source position is occupied at any given time. The source remains parallel to the plane of the collimator throughout the procedure.

pinholes using the same geometry as described in Section III A with a separation of 6.5 mm (centre to centre) was simulated. The configuration is shown in Figure 7. The source was placed at a distance of 5 mm from the upper surface of the collimator at the midpoint of the two pinholes and parallel to the Y axis on which the pinholes lie. Ten billion photon events were simulated, and the location of the centres of mass of the resulting projections through adjacent pinholes were evaluated. These were then used to estimate the source position.

To estimate the error in calculating the source position within the prostate volume (i.e. simulating an error in source position in the X-Z and Y-Z planes), a second pinhole was simulated, with the source occupying the same positions as shown in Figure 6. The projection images through the second pinhole were used in conjunction with those acquired in the single pinhole studies to estimate the source position within the prostate volume. The error between the estimated and actual (simulated) source position was then calculated.

14
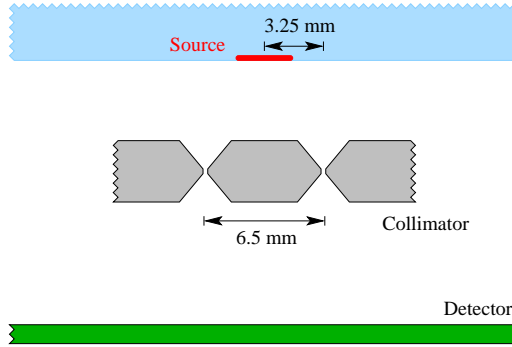
FIG. 7. Monte Carlo simulation set up for the double pinhole study.

IV. RESULTS

The projected images of the source placed in the positions described in Section III A through the single pinhole are shown in Figure 8. The image intensity corresponds to the number of counts recorded in each pixel. The range of counts is shown in the colourbar adjacent to each image.

The lowest count rates occur when the source is placed at the maximum distance from the detector (Figure 8(h)), with a maximum of 17 counts per pixel recorded for the 20 billion photons generated by the source. While the source can be resolved in each of the simulated positions, a high background count occurs due to large number of *penetrated photons*, which contributes to a degradation in signal to background ratio (SBR). The SBR is at its minimum when the source is placed closest to the edge of FoV ($\theta = 57°$). This is as expected, since the ratio of penetrated photons to direct photons is at its maximum. The projection image corresponding to the source at this position is shown in Figure 8(c); although the SBR is clearly at its lowest compared to other simulated positions, the centre of mass of the projected image can still be accurately determined. The theoretically calculated centre of mass (corresponding to projection of the source through an infinitely attenuating collimator) and the measured positions of the centre of mass of source projections are marked with a red x and a blue + respectively.

The error in estimating the location of the calculated centre of mass of the projected source (blue +) compared to its theoretical position (red x) is shown in Table II. The X and Y axes are identical to those shown in Figure 1. The maximum error (in the detector plane) in the X direction (dx) is approximately 0.055 mm, which is within the intrinsic resolution

(a)$h = 7$mm, $\theta = 90°$ (b)$h = 7$mm, $\theta = 72°$ (c)$h = 7$mm, $\theta = 57°$

(d)$h = 23$mm, $\theta = 90°$ (e)$h = 23$mm, $\theta = 72°$ (f)$h = 23$mm, $\theta = 57°$

(g)$h = 47$mm, $\theta = 90°$ (h)$h = 47$mm, $\theta = 72°$
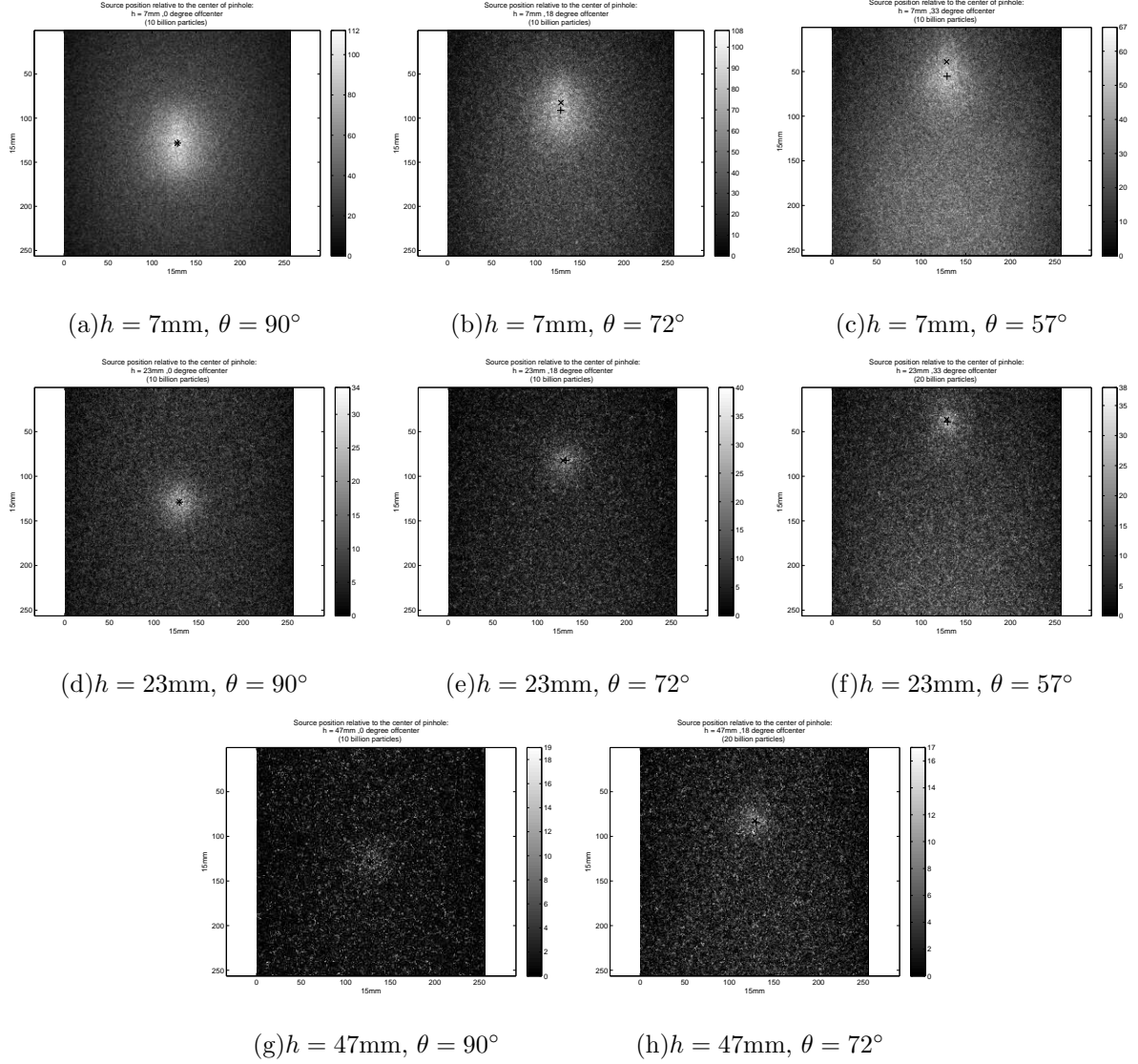
FIG. 8. Simulated projection images of a single pinhole collimator and source in 8 different positions within the FoV. h is the perpendicular distance between source and the pinhole centre and θ is the incidence angle measured from the pinhole plane (Figure 6). The theoretically calculated and measured positions of the centre of mass of source projections are marked with a red x and a blue + respectively.

of detector. The maximum error in the Y direction (dy) occurs when the source is closest to the pinhole ($h = 7$ mm) and at the edge of its FoV, and is approximately 0.945 mm.

Figure 9 shows the source projection image through two adjacent pinholes as discussed in Section III B. As there is a clear separation of the two projections, it is possible to correctly estimate the respective centres of mass of each projection.

16

TABLE II. Error of estimated centre of mass on detector plane for the source in different positions.

Source position	dx in detector plane (mm)	dy in detector plane (mm)
$h = 7.21$ mm, $\theta = 90°$	0.026	-0.012
$h = 7.21$ mm, $\theta = 82°$	-0.014	0.509
$h = 7.21$ mm, $\theta = 67°$	0.028	0.945
$h = 23.14$ mm, $\theta = 90°$	0.009	0.027
$h = 23.14$ mm, $\theta = 82°$	0.191	-0.013
$h = 23.14$ mm, $\theta = 67°$	0.055	0.155
$h = 47.21$ mm, $\theta = 90°$	-0.062	0.034
$h = 47.21$ mm, $\theta = 82°$	0.075	0.107
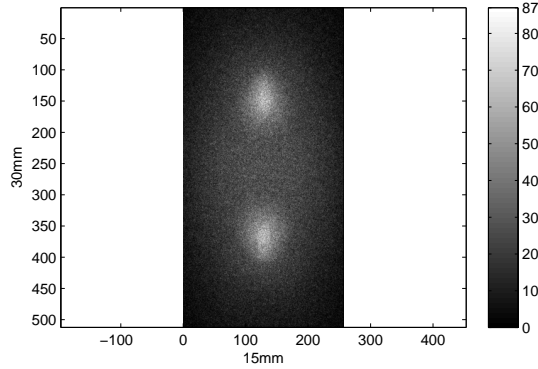
FIG. 9. Simulation of double pinhole collimator; the distance between the pinholes is 6.5 mm (centre to centre) and the source is placed 5 mm above the collimator and aligned with the axis joining the two pinholes.

The calculated error in resolving the centre of the reconstructed source placed at different positions within the prostate volume is listed in Table III.

V. DISCUSSION

The projections observed in the single pinhole simulation (shown in Figure 8) demonstrates that the SBR deteriorates at the edge of the FoV, with a minimum peak value of 17 counts detected for the projected image of the source for 20 billion simulated photons. How-

17

TABLE III. Estimated difference in reconstructed and pre-defined source locations within the prostate phantom.

Source position	dx (mm)	dy (mm)	dz (mm)	$\sqrt{dx^2 + dy^2 + dz^2}$ (mm)
$h = 7.21$ mm, $\theta = 82°$	0.014	-0.053	1.475	1.476
$h = 7.21$ mm, $\theta = 67°$	0.020	-0.114	1.367	1.372
$h = 23.14$ mm, $\theta = 90°$	0.001	-0.075	-0.358	0.366
$h = 23.14$ mm, $\theta = 82°$	0.262	-0.248	-0.933	1.001
$h = 23.14$ mm, $\theta = 67°$	0.168	-0.057	0.593	0.619
$h = 47.21$ mm, $\theta = 90°$	-0.280	-0.189	-0.127	0.361
$h = 47.21$ mm, $\theta = 82°$	0.468	-0.290	1.030	1.168

ever, given that the typical activity of the ^{192}Ir sources used in HDR prostate brachytherapy is around 370 GBq (corresponding to a photon flux of 870 billion photons per second), it is reasonable to predict that HDR BrachyView system is capable of resolving the source within a sub-second dwell time. Therefore, the system is suitable for real-time source tracking.

The uncertainty values listed in Table II demonstrate that the maximum source positioning error on detector plane in the X direction is less than the intrinsic spatial resolution of the detector. The maximum error in resolving the centre of mass of the source projection in the Y direction is 0.945 mm. This shift is due to the asymmetry of pinhole sensitivity with respect to the point of origin of emitted photons along the longitudinal axis of the source. The sensitivity of a pinhole collimator S_t is defined as the fraction of photons emitted from a point source that reach the camera detector, and is the sum of the "direct" (S_d) and "penetrative" (S_p) sensitivities:

$$S_t(\theta) = S_d(\theta) + S_p(\theta) \tag{1}$$

where θ is the incidence angle of photons on the pinhole plane. For an aperture with a pinhole diameter of d, the direct sensitivity calculated for a point source placed at a distance h from the pinhole plane is given by[23]:

$$S_d(\theta) = \frac{d^2 \sin^3(\theta)}{16h^2} \tag{2}$$

The penetrative term can be analytically determined by calculating the path length of

18
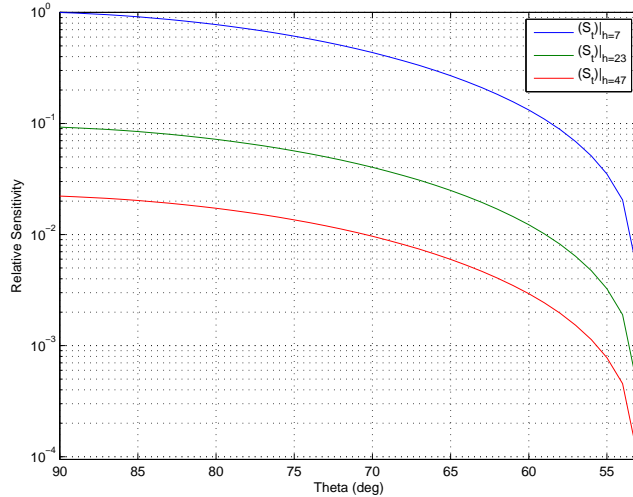
FIG. 10. Analytical estimate of HDR BrachyView pinhole sensitivity (with penetration) versus *theta* using an ^{192}Ir point source with tungsten collimator, normalised to 1 at $\theta = 90°$ and $h = 7$ mm.

incident photons through the collimator from an ideal point source and then integrating the attenuated flux over all points constituting a line source such as an ^{192}Ir seed[24]. Furthermore, the penetrative sensitivity can be further approximated, assuming that photons with an incident angle of $\theta < (\pi - \alpha)/2$ are mostly stopped due to the large volume of material they traverse[24]. Therefore, for a pinhole collimator with an opening angle of α and a diameter of d:

$$S_p(\theta) \approx \frac{\sin^5 \theta \tan^2 \frac{\alpha}{2}}{8h^2\mu^2} \times \left(1 - \frac{\cot^2 \theta}{\tan^2 \frac{\alpha}{2}}\right)^{1/2} \times \left[1 - \frac{\cot^2 \theta}{\tan^2 \frac{\alpha}{2}} + \mu d \csc \theta \cot \frac{\alpha}{2}\right] \qquad (3)$$

The theoretical relative sensitivity of the HDR BrachyView pinhole is plotted for a point source placed at different heights above the collimator (normalised for $h = 7$ mm and $\theta = 90°$) and is shown in Figure 10. When the source is placed 7 mm above the pinhole, θ varies from 58° to 74° for photons emitted along the Y-axis, resulting in an 84% variation in sensitivity across the length of the source. The predicted relative reduction in the total sensitivity for different source positions based on the analytic model is in good agreement with the results of the Monte Carlo simulations presented in Section IV.

The non-uniform distortion of the pinhole response function in the Y direction for a linear brachytherapy source is illustrated in Figure 11. As the source is moved along the Y axis

19
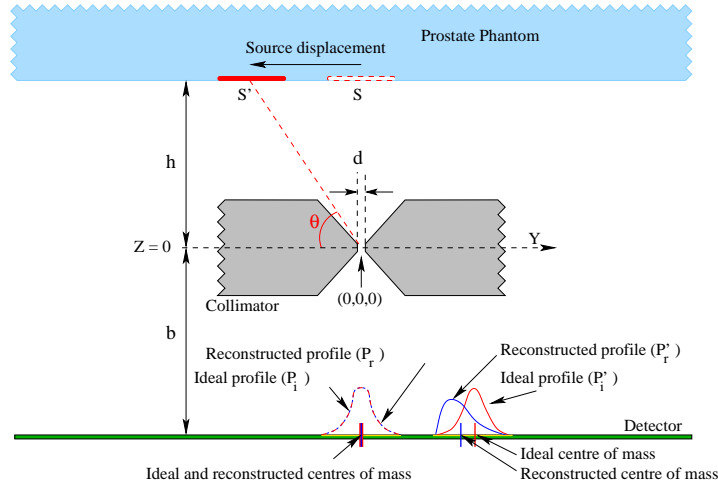
FIG. 11. Geometry for asymmetric projection: Ideal centre projection is a reference position defined as the projection of source centre on detector through the centre of pinhole. The projection image centre is the centre position calculated from the image.

(from position S to S'), its inverted projection moves in the opposite direction. While the Y-axis projection profile is symmetric at normal incidence angle ($\theta = 90°$), the reconstructed source profile is significantly distorted when the source is moved along the Y axis, with its centre of mass moving towards the pinhole. Since the variation of the relative sensitivity along the longitudinal source axis is inversely proportional to the square of the distance between the source and the pinhole (h^2), the error in the centre of mass (on the detector plane) also decreases with the increased source to pinhole distance.

The error in resolving the location of the source within the prostate volume varies between 0.361 mm (where the source is directly above the collimator) and 1.476 mm (when the source is at the edge of the field of view). While the error is significant, it is worth noting that it was only calculated based on two projections, where as in reality, there will be seven projections for source placed at that distance. This will ultimately result in a more accurate estimation of the centre of mass of the source. Furthermore, the error clearly includes a component which is clearly a function of source position; this is due to the fact that the centre of mass of the projected image is not quite perfectly aligned with the ideal point of intersection of the line projected from the centre of the source. Therefore it will be possible to develop a model for the error as a function of position, either via simulation or experimentally using a calibration procedure, which can correct for this systemic component of the error. This

20

issue will be addressed in the next phase of research.

VI. CONCLUSION

The HDR BrachyView probe is an in-body pinhole imaging system designed for real time source localisation during prostate HDR brachytherapy procedures. The position of ^{192}Ir source centre can be calculated from multiple images projected on an array of Timepix detectors through a series of pinholes in a tungsten collimator over the dwell time of the source. Several sets of GEANT4 simulations have been performed to validate the design. These simulations show that there is a small shift toward the perpendicular projection of pinhole centre on the detector plane in each image, which is a result of the asymmetry of the projected image when the source is not placed directly above the pinhole. The simulation results show that the errors in estimating the centre of mass of the projection in the detector plane do not exceed 1 mm in the worst case, and that the positioning error decreases when source is placed further away from the collimator. The simulated double pinhole studies estimated the maximum error in estimating the source position within the prostate volume to be 1.5 mm. A prototype of the HDR BrachyView system is currently under development. Experimental studies with a prototype collimator and HDR source are currently being performed in a phantom to validate the simulation results; these will be the subject of a separate paper. In future work, the effect of backscatter associated with the introduction of the HDR Brachytherapy rectal in-body imaging probe on the total dose received by the rectal wall will be evaluated both in simulation and experimentally.

* Email: anatoly@uow.edu.au; A.B. Rosenfeld

21

[1] N. Howlader, A.M. Noone, M. Krapcho, N. Neyman, R. Aminou, S.F. Altekruse, C.L. Kosary, J. Ruhl, Z. Tatalovich, H. Cho, A. Mariotto, M.P. Eisner, D.R. Lewis, H.S. Chen, E.J. Feuer, and K.A. Cronin, *SEER Cancer Statistics Review, 1975-2009 (Vintage 2009 Populations)*, Tech. Rep. (National Cancer Institute, 2012) `http://seer.cancer.gov/csr/1975_2009_pops09/`.

[2] M. Batic, J. Burger, V. Cindro, G. Kramberger, I. Mandic, M. Mikuz, A. Studen, and M. Zavrtanik, "Verification of High Dose Rate Ir-192 Source Position During Brachytherapy Treatment Using Silicon Pixel Detectors," IEEE T Nucl Sci **58**, 2250–2256 (2011).

[3] D. Sheikh-Bagheri and P. Munro, "A Monte Carlo study of verification imaging in high dose rate brachytherapy," Med Phys **25**, 404–414 (1998).

[4] B. Thomadsen, S.W. Lin, P. Laemmrich, T.Waller, A. Cheng, B. Caldwell, R. Rankin, and J. Stitt, "Analysis of treatment delivery errors in brachytherapy using formal risk analysis techniques," Int J Radiat Oncol **57**, 1492–1508 (2003).

[5] L. Sullivan, S. Williams, K. Tai, F. Foroudi, L. Cleeve, and G. Duchesne, "Urethral structure following high dose rate brachytherapy for prostate cancer," Radiother Oncol **91**, 232–236 (2009).

[6] C. Buron, B. Le Vu, and J.M. Cosset et al., "Brachytherapy versus prostatectomy in localized prostate cancer: Results of a French multicenter prospective medico-economic study," Int J Radiat Oncol **67**, 812–822 (2007).

[7] J. Lambert, T. Nakano, S. Law, J. Elsey, D.R. McKenzie, and N. Suchowerska, "In vivo dosimeters for HDR brachytherapy: a comparison of a diamond detector, MOSFET, TLD, and scintillation detector," Med Phys **34**, 1759–1765 (2007).

[8] Z. Qi, X. Deng, S. Huang, J. Lu, M. Lerch, D. Cutajar, and A. Rosenfeld, "Verification of the plan dosimetry for high dose rate brachytherapy using metal-oxide-semiconductor field effect transistor detectors," Med Phys **34**, 2007–2013 (2007).

[9] E.L. Seymour, S.J. Downes, G.B. Fogarty, M.A. Izard, and P. Metcalfe, "In vivo real-time dosimetric verification in high dose rate prostate brachytherapy," Med Phys **38**, 4785–4794 (2011).

[10] I.S. Kwan, D. Wilkinson, D. Cutajar, M. Lerch, A. Rosenfeld, A. Howie, J. Bucci, Y. Chin, and V.L. Perevertaylo, "The effect of rectal heterogeneity on wall dose in high dose rate brachytherapy," Med Phys **36**, 224–232 (2009).

[11] N. Suchowerska, J. Lambert, T. Nakano, S. Law, J. Elsey, and D.R. McKenzie, "A fibre optic dosimeter customised for brachytherapy," Radiat Meas **42**, 929–932 (2007).

[12] L.W. Cartwright, N. Suchowerska, Y. Yin, J. Lambert, M. Haque, and D.R. McKenzie, "Dose mapping of the rectal wall during brachytherapy with an array of scintillation dosimeters," Med Phys **37**, 2247–2255 (2010).

[13] N. Suchowerska, M. Jackson, J. Lambert, Y. Bai Yin, G. Hruby, and D. R. McKenzie, "Clinical Trials of a Urethral Dose Measurement System in Brachytherapy Using Scintillation Detectors," Int J Radiat Oncol **79**, 609–615 (2011).

[14] L. Archambault, T. M. Briere, F. Pönisch, L. Beaulieu, D. A. Kuban, A. Lee, and S. Beddar, "Toward a Real-Time In Vivo Dosimetry System Using Plastic Scintillation Detectors," Int J Radiat Oncol **78**, 280–287 (2010).

[15] J. Duan, D.J. Macey, P.N. Pareek, and I.A. Brezovich, "Real-time monitoring and verification of in vivo high dose rate brachytherapy using a pinhole camera," Med Phys **28**, 167–173 (2001).

[16] H. Song, J. Bowsher, S. Das, and F. Yin, "Tracking brachytherapy sources using emission imaging with one flat panel detector," Med Phys **36**, 1109–1111 (2009).

[17] J. Dammera, P.M. Frallicciardib, J. Jakubeka, M. Jakubeka, S. Pospisila, E. Prenerovac, D. Vavrika, L. Volterd, F. Weydad, and R. Zemekd, "Real time in vivo imaging with Medipix2," Nucl Instrum Meth A **607**, 205–207 (2009).

[18] X. Llopart2, M.Campbell, D. San Segundo, E. Pernigotti, and R. Dinapoli, "Medipix2, a 64k pixel read out chip with 55 μm square elements working in single photon counting mode," in *IEEE Nucl Sci Conf R*, Vol. 3 (IEEE, 2001) pp. 1482–1488.

[19] R. Accorsi and S.D. Metzler, "Analytic determination of the resolution-equivalent effective diameter of a pinhole collimator," IEEE T Med Imaging **23**, 750 –763 (Jun. 2004).

[20] R. Accorsi and S.D. Metzler, "Resolution-effective diameters for asymmetric-knife-edge pinhole collimators," IEEE T Med Imaging **24**, 1637 –1646 (Dec. 2005).

[21] F. van der Have and F.J. Beekman, "Photon penetration and scatter in micro-pinhole imaging: a Monte Carlo investigation," Phys Med Biol **49**, 1369–1386 (2004)).

[22] D. Rogers, *Monte Carlo models of Ir-192 sources*, National Research Council of Canada Ottawa (1999).

[23] H.O. Anger and D.J. Rosenthal, "Scintillation camera and positron camera," Medical Radioisotope Imaging, 59–75(1959).

[24] S.D. Metzler, J.E. Bowsher, M.F. Smith, and R.J. Jaszczak, "Analytic determination of pinhole collimator sensitivity with penetration," IEEE T Med Imaging **20**, 730 –741 (Aug. 2001).